Materials Transactions, Vol. 48, No. 11 (2007) pp. 2809 to 2815
Special Issue on Structural and Functional Control of Materials through Solid-Solid Phase Transformations in High Magnetic Fields

Effect of High Magnetic Field Annealing on Microstructure and Texture at the Initial Stage of Recrystallization in a Cold-Rolled Interstitial-Free Steel

Yan Wu[1,*1], Xiang Zhao[1,*2], Chang-Shu He[1], Yu-Dong Zhang[1], Liang Zuo[1] and Claude Esling[2]

[1]*Key Laboratory for Anisotropy and Texture of Materials (Ministry of Education), Northeastern University, Shenyang 110004, P. R. China*
[2]*LETAM, CNRS-UMR 7078, University of Metz, Ile du Saulcy, 57045 Metz, Moselle, France*

The effects of magnetic field annealing on microstructure and texture evolution at the initial stage of recrystallization in as-annealed interstitial-free (IF) steel sheet were investigated by the orientation imaging microscopy (OIM) and microhardness testing. The magnetic field annealing was conducted in a 12-tesla magnetic field at 650°C for different time spans (0, 10 and 30 min) to obtain partially recrystallized microstructure in specimens. It was found that the magnetic field annealing retarded the recrystallization process, and favoured the development of ⟨110⟩ texture components at the initial stage of recrystallization. Additionally, it is worth noting that, in the case of annealing for 10 min, we observed more pronounced {111}⟨123⟩ component associated with coarse grains in the magnetic field annealed specimen, which may suggest that this component was favoured by the applied high magnetic field in the early stage of nucleation and growth.
[doi:10.2320/matertrans.MI200707]

(Received May 1, 2007; Accepted July 9, 2007; Published October 25, 2007)

Keywords: *high magnetic field, texture, recrystallization, nucleation, orientation imaging microscopy (OIM), interstitial-free (IF) steel*

1. Introduction

As an important external field, it has been evidenced experimentally that magnetic field can affect the development of recrystallization and recrystallization texture in plastically deformed metallic materials,[1–9] especially in ferromagnetic materials.[1–7] While for ferromagnetic materials, the study of magnetic field annealing on recrystallization and texture evolution in silicon steel sheet and IF deep-drawing steel sheet has been an object of great attention. As reported else where,[6,7] the research work of high magnetic field annealing on recrystallization and texture evolution in IF steel sheet was mainly focused on the grain growth stage, by changing the annealing temperatures at a range of 650∼850°C, and the holding time at an annealing temperature (750°C) near Curie point. The results show that the recrystallization and the subsequent grain growth were retarded by the magnetic field annealing, and the recrystallization texture development was retarded to some extent, too. However, there are still several interesting issues remain to be studied. Undoubtedly, much work is still required to understand the underlying mechanism of high magnetic field inducing crystal orientation during the stage of nucleation and growth in IF steel sheet. So in the present paper, we particularly report the effects of high magnetic field annealing on microstructure and recrystallization texture in a cold-rolled IF steel sheet at the initial stage of recrystallization.

2. Experimental

The material used was a 76% cold-rolled IF steel sheet of 1 mm thickness, having the chemical composition of (mass%): 0.0023C, 0.056Ti, 0.014Si, 0.16Mn, 0.011P, 0.0064S, 0.052Al, 0.0018N. Specimens with the dimensions of 20 mm × 10 mm × 1 mm were respectively subjected to isothermal annealing at 650°C for different time (0, 10 and 30 min) in a furnace installed in a cryocooler-cooled superconducting magnet at a heating rate of 5°C/min, with and without a 12-tesla magnetic field, and then cooled in the furnace. During the magnetic field annealing, a magnetic field was kept being applied in the whole heating and cooling processes. The specimens were placed at the center of the applied field with their rolling direction (RD) paralleling to the magnetic field direction (MD). The experimental setup is schematically shown in Fig. 1.

Microstructures of longitudinal sections of the specimens were examined by orientation imaging microscopy (OIM). In the maps, the recrystallized grains are highlighted (dark grains). The scan was carried out over the area of 1191 × 878 measuring points with a 0.07 μm step size, and the corresponding ODFs were calculated using the Channel 5

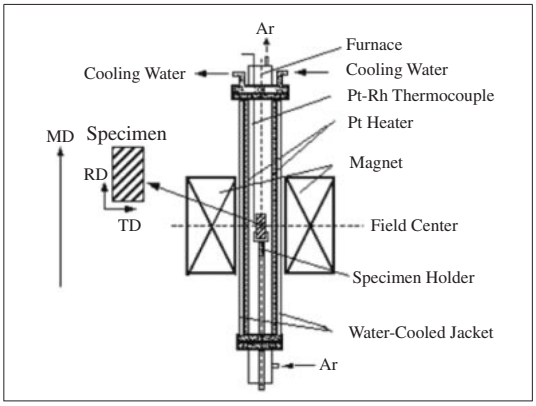

Fig. 1 Schematic illustration of high magnetic field annealing equipment.

*1Graduate Student, Northeastern University
*2Corresponding author, E-mail: zhaox@mail.neu.edu.cn

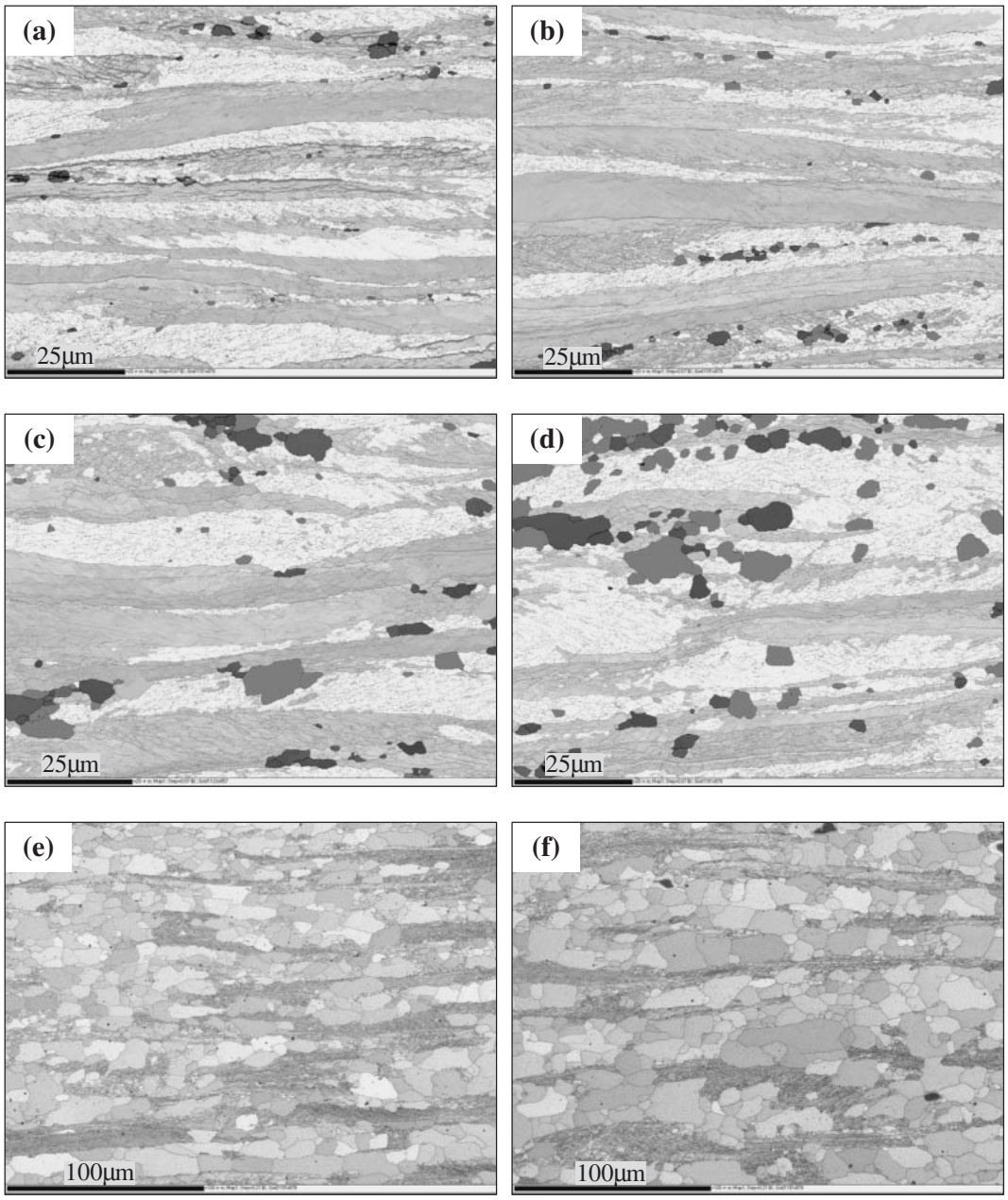

Fig. 2 OIM (Band Contrast + Texture Component) maps of specimens annealed at 650°C: white color regions: γ texture components; (a) 12 T × 0 min; (b) 0 T × 0 min; (c) 12 T × 10 min; (d) 0 T × 10 min; (e) 12 T × 30 min; (f) 0 T × 30 min.

software. The microhardness of the annealed specimens was made on their longitudinal sections with 50 g load and a holding time of 15 s. The average microhardness of each specimen was taken from 10 measurements.

3. Results and Discussion

3.1 Effects of high magnetic field annealing on microstructure evolution

Figure 2 shows the microstructures of longitudinal sections of the specimens annealed at 650°C holding for different time. In these OIM maps, both the rolling direction and the magnetic field direction are horizontal. The {111} oriented deformation bands (white color regions) in the maps are plotted with 15° orientation spread from the exact {111} orientation. The relatively dark grains in Figs. 2(a), (b), (c), (d) are the recrystallized nuclei and grains, which are surrounded by grain boundaries with misorientation over 10° and the misorientation in regions is less than 1°. As Figs. 2(a) and (b) show, in the case of holding for 0 min, there are many strong deformation bands retained in both the field and non-field annealed specimens, and only limited recrystallized nuclei can be observed among the {111} oriented deformation bands. When the holding time is 10 min (Figs. 2(c) and (d)), the retained deformation bands in the non-field annealed specimen are much smaller than in the field annealed specimen, correspondingly, the number of recrystallized nuclei in the former is also much more than the latter. Besides, from Figs. 2(c) and (d) we also can see that the recrystallized nuclei in both the field and non-field annealed specimens nucleated in {111} oriented deformation bands, which is also found in the work of Quadir[10] and

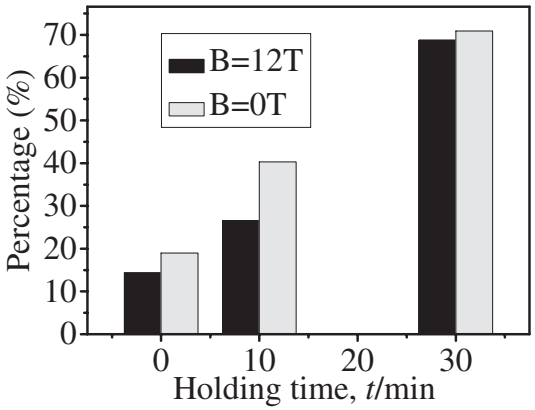

Fig. 3 Area percentage of recrystallized regions in the specimens annealed at 650°C.

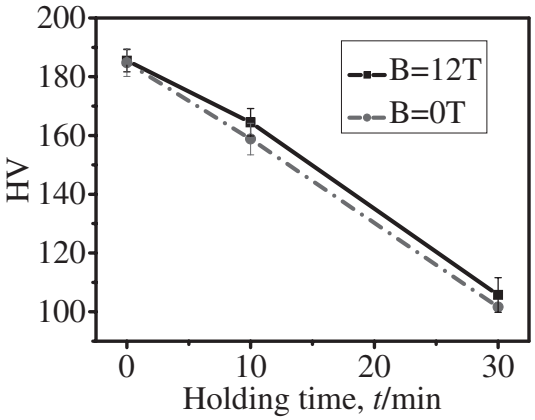

Fig. 4 Microhardness of the specimens annealed at 650°C.

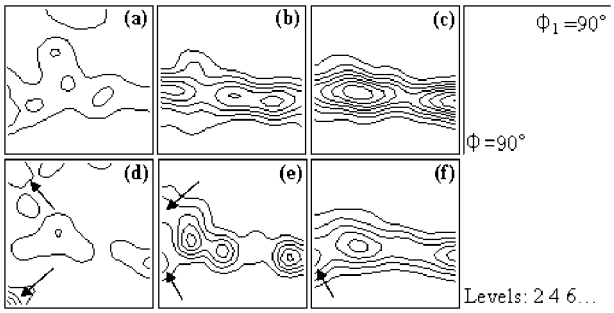

Fig. 5 ODF $\Phi_2 = 45°$ sections for the recrystallized grains of the specimens annealed at 650°C: (a) 0 T × 0 min; (b) 0 T × 10 min; (c) 0 T × 30 min; (d) 12 T × 0 min; (e) 12 T × 10 min; (f) 12 T × 30 min.

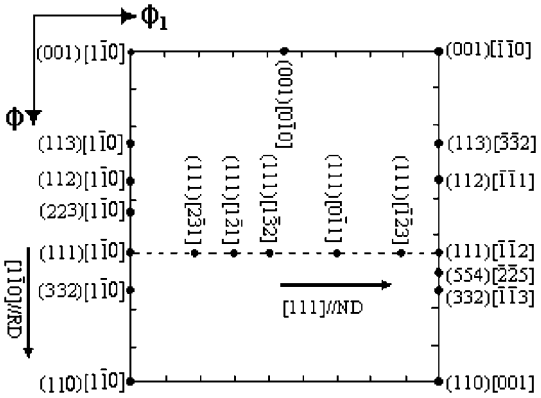

Fig. 6 $\Phi_2 = 45°$ sections of the ODF for bcc metals. (Bunge system)

Tse,[11] since the deformed {111} orientations display higher stored energy and fairly sharp orientation gradient, and are capable of providing the necessary geometrical conditions for nucleation and recrystallization. When the annealing time was further extended to 30 min, a lot of recrystallized grains appear in the annealed specimens, but the recrystallized grains in non-field annealed specimen are much larger than those in the field annealed specimen, as seen in Figs. 2(e) and (f). The quantitative comparison of their area percentage of recrystallized regions is shown in Fig. 3. It is obvious that the area percentage of recrystallized regions in all field-annealed specimens is lower than in the corresponding non-field annealed specimens. This is accordance with the microhardness results shown in Fig. 4. It is evident that, with the increasing of holding time, the microhardness of both field and non-field annealed specimens decreased remarkably, but the microhardness of field-annealed specimens is all higher than that of the corresponding non-field annealed specimens. The above results indicate that the magnetic field retards the recrystallization process.

So far, how a high magnetic field influences recrystallization is still unclear. As pointed elsewhere,[12–15] the possible mechanisms might be related to magnetically ordered state and domain wall rearrangement induced by magnetic field, which are considered as two main factors affecting atomic diffusion and grain boundary migration. Anyway, for iron-based alloys, the retardation of recrystallization by magnetic field application is known as a common feature of magnetic field annealing.[16]

3.2 Effects of high magnetic field annealing on texture evolution

Figure 5 shows the ODF $\Phi_2 = 45°$ sections of all recrystallized grains in annealed specimens holding for different time. Figure 6 displays the ODF $\Phi_2 = 45°$ section of Bunge's Euler space and the major orientation components along the α ($\langle 110 \rangle$ // RD) and γ ($\langle 111 \rangle$ // ND) fibers. As Figs. 5(a) and (d) show, in the case of holding for 0 min, the orientation of recrystallized nuclei determined in the non-field annealed specimen is mainly {111}⟨uvw⟩, while it is a little different for the field annealed specimen, *i.e.* the orientation of the recrystallized nuclei is mainly consist of strong {110}⟨110⟩ and weak {111}⟨uvw⟩ components. In the case of holding for 10 min, the recrystallized grains in non-field annealed specimen exhibit a strong γ fiber texture with intensity peaks between {111}⟨123⟩ and {111}⟨110⟩ (Fig. 5(b)), while for the field annealed specimen, the orientation of the recrystallized grains mainly have strong {111}⟨123⟩ and weak {hkl}⟨110⟩ textures (Fig. 5(e)). When the annealing time was further extended to 30 min, the orientations distribution of recrystallized grains in field and non-field annealed specimens display similar morphologies with intensity peak at {111}⟨112⟩ (Fig. 5(c), (f)), while for the field annealed specimen, the intensity of {111}⟨112⟩ component is relatively lower than that of the non-field

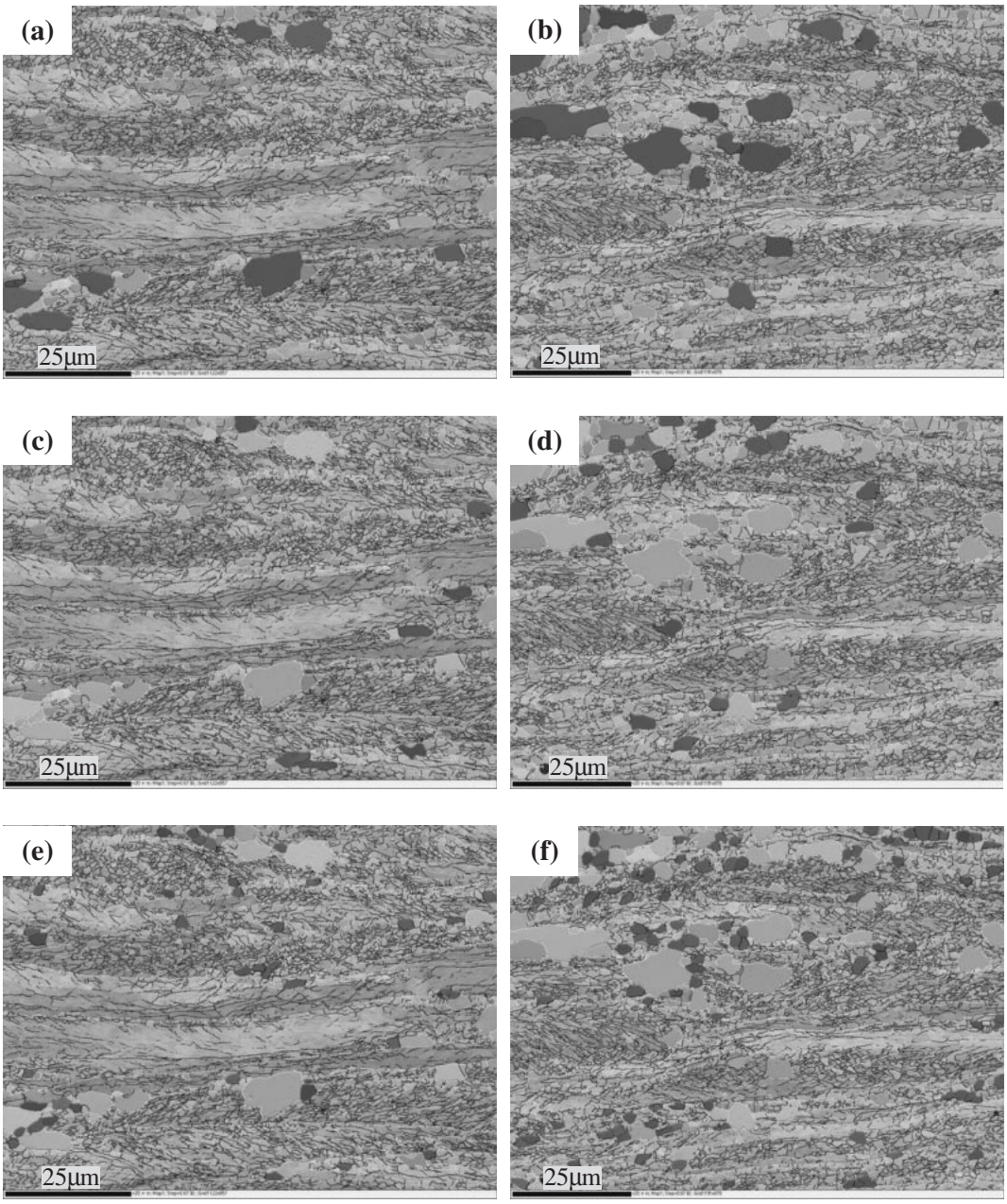

Fig. 7 OIM (Band Contrast + Grain boundary) maps of annealed specimens holding for 10 min: (a) 12 T × 10 min, large grains; (b) 0 T × 10 min, large grains; (c) 12 T × 10 min, medium grains; (d) 0 T × 10 min, medium grains; (e) 12 T × 10 min, small grains; (f) 0 T × 10 min, small grains. (Black lines $\leq 5^\circ$, $5^\circ <$ red lines $\leq 10^\circ$, and white lines $> 10^\circ$ misorientation; large grains(area) $\geq 10\,\mu m^2$, $6\,\mu m^2 \leq$ medium grains (area) $< 10\,\mu m^2$, $2\,\mu m^2 \leq$ small grains (area) $< 6\,\mu m^2$).

annealed specimen. In addition, a texture component of {443}⟨110⟩, which belongs to the α fiber, is observed for the field annealed specimen. Arrows in Figs. 5(d), (e) and (f) show the {hkl}⟨110⟩ texture components determined in the field annealed specimens which are not visible in the ODFs of the non-field annealed specimens. The above results obviously indicate that high magnetic field annealing favoured the development of ⟨110⟩ texture components at the initial stage of recrystallization.

It is known that Magnetic field could lower the Gibbs free energy of differently orientated grains according to their magnetization. As a sequence, the changes of magnetic field free energy (ΔG) affecting grains with ⟨100⟩, ⟨110⟩ and ⟨111⟩ orientations parallel to the direction of the magnetic field (MD) can be written in the following sequence:[13)]

$$|\Delta G_{\langle 111\rangle}| < |\Delta G_{\langle 110\rangle}| < |\Delta G_{\langle 100\rangle}| \quad (1)$$

Obviously, the free energy of the grains with ⟨100⟩ orientation parallel to the magnetic field is the lowest, and they have the largest driving force for recrystallization, then the ⟨110⟩ oriented grains, and the ⟨111⟩ oriented grains. While for the IF steel sheet investigated in this study, no measurable orientation intensity at {hkl}⟨100⟩ was determined before and after annealing, which suggests that nucleation of grains with ⟨110⟩ orientation become the most preferred during magnetic field annealing. Therefore, when the magnetic field direction parallel to the specimens' rolling direction, at the initial stage of recrystallization, the ⟨110⟩

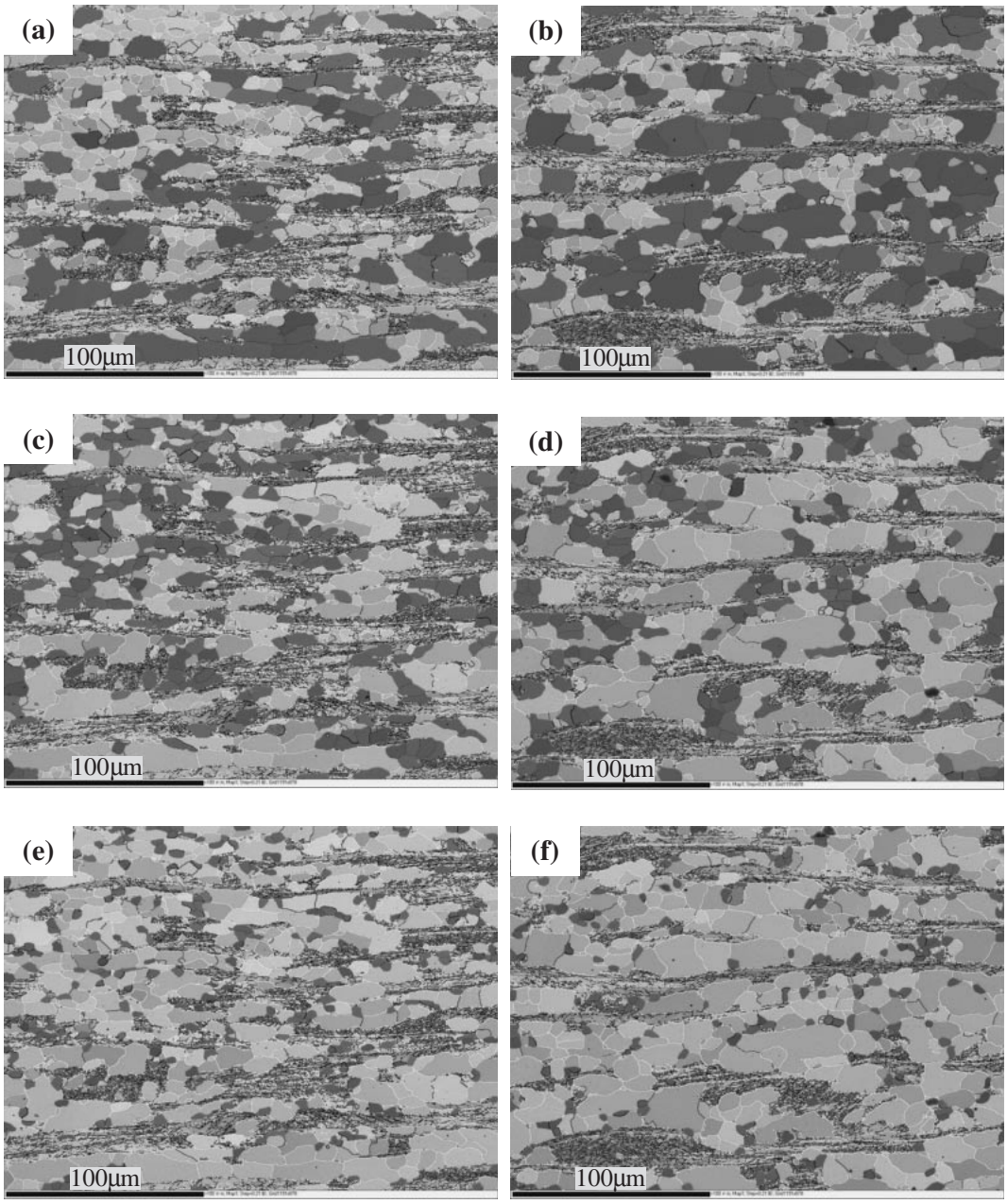

Fig. 8 OIM (Band Contrast + Grain boundary) maps of annealed specimens holding for 30 min: (a) 12 T × 30 min, large grains; (b) 0 T × 30 min, large grains; (c) 12 T × 30 min, medium grains; (d) 0 T × 30 min, medium grains; (e) 12 T × 30 min, small grains; (f) 0 T × 30 min, small grains. (Black lines $\leq 5^\circ$, $5^\circ <$ red lines $\leq 10^\circ$, and white lines $> 10^\circ$ misorientation; large grains (area) $\geq 100\,\mu m^2$, $30\,\mu m^2 \leq$ medium grains (area) $< 100\,\mu m^2$, $10\,\mu m^2 \leq$ small grains(area) $< 30\,\mu m^2$).

oriented nuclei are considered to be energetically favored, which make the nucleation and growth of ⟨110⟩ oriented nuclei in field annealed specimens become easier than that in the non-field annealed specimens. Besides, the selected annealing temperature of 650°C is slightly over the recrystallization temperature and lies within the ferromagnetic temperature range far from the Curie point, which might make the preferred orientation mechanism induced by magnetic free energy anisotropy play an important role in recrystallization nucleation.

We further investigated orientation features among the large, medium and small recrystallized grains in field and non-field annealed specimens. Figure 7 and Figure 8 show the OIM (Band Contrast + Grain boundary) maps of annealed specimens holding for 10 and 30 min, respectively. The dark color grains in the maps are the recrystallized grains with different size. The corresponding ODF $\Phi_2 = 45^\circ$ sections of those recrystallized grains are shown in Fig. 9. It can be seen that, in the case of holding for 10 min without field (Fig. 9(a)), the {111}⟨110⟩, {111}⟨123⟩ and {111}⟨112⟩ orientations are respectively associated with the large, medium and small recrystallized grains. However, it is obviously different when applying the high magnetic field. After holding for 10 min in high magnetic field (Fig. 9(b)), the large recrystallized grains display a much stronger texture at {111}⟨123⟩ orientation. The medium and the small recrystallized grains exhibit much weak textures, with intensity peak at {111}⟨123⟩ and {111}⟨112⟩, respectively.

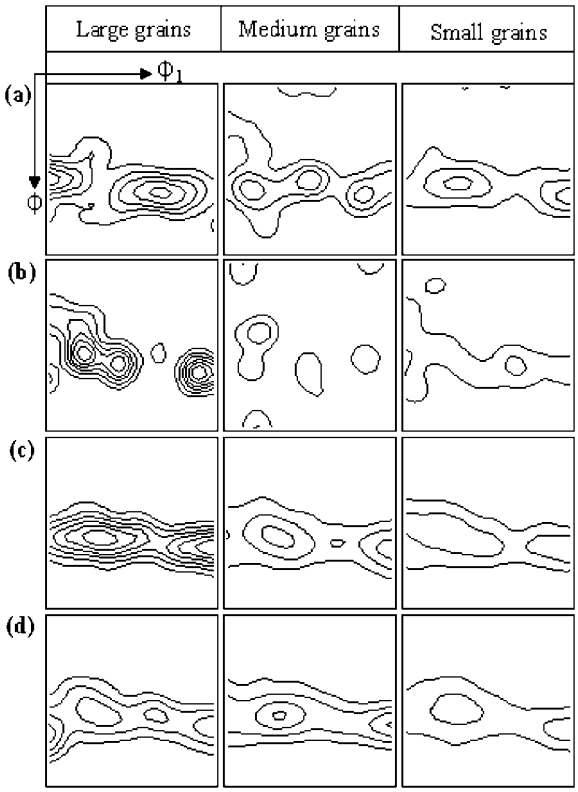

Fig. 9 ODF $\Phi_2 = 45^\circ$ sections of different size recrystallized grains in annealed specimens holding for 10 and 30 min, respectively: (a) 0 T × 10 min; (b) 12 T × 10 min; (c) 0 T × 30 min; (d) 12 T × 30 min.

When the holding time is 30 min (Fig. 9(c), (d)), all the recrystallized grains with different size determined in field and non-field annealed specimens exhibit a γ-fiber texture with intensity peak at $\{111\}\langle 112\rangle$.

In cold-deformed IF steel sheet, $\{111\}\langle 110\rangle$, $\{111\}\langle 123\rangle$ and $\{111\}\langle 112\rangle$ are the main texture components of γ-fiber texture. According to the research work of Takechi *et al.*[17] and Rajmohan *et al.*[18] on the stored energy in particular orientations in cold rolled IF steel, the stored energy in the deformed regions of $\{111\}\langle 112\rangle$ orientation is higher than that in the regions of $\{111\}\langle 110\rangle$ and $\{111\}\langle 123\rangle$ orientations. Consequently, nucleation occurs in $\{111\}\langle 112\rangle$ oriented deformed matrix is considered to be energetically favored. Additionally, in iron,[19] $\{111\}\langle 110\rangle$ oriented crystals have a better $30^\circ\langle 111\rangle$ orientation relationship with $\{111\}\langle 112\rangle$ oriented matrix ($\sum$13b CSL grain boundary). In general terms, $\sum$ CSL grain boundaries have lower interface energy than random grain boundaries. So, at the initial stage of recrystallization, $\{111\}\langle 110\rangle$ oriented nuclei will prefer to grow in $\{111\}\langle 112\rangle$ oriented deformation matrix. Based on the above discussions, it is reasonable to speculate that the $\{111\}\langle 110\rangle$ oriented nuclei are very likely to develop into coarse grains with the same orientation in a certain recrystallization stage. In the present study, the case of the non-field annealed specimen displays strong $\{111\}\langle 110\rangle$ texture associate with large grains after holding for 10 min (Fig. 9(a)), which implies that this component nucleate earlier and have more time to grow as compared with other texture components. In the case of magnetic field annealing, the coarse grains are of strong $\{111\}\langle 123\rangle$ texture component, which suggests that the nucleation and growth of this component are favored by the applied high magnetic field during the initial stage of recrystallization.

It is known that, when applying a high magnetic field, the change of Gibbs energy of a grain depends on its orientation. Generally, the magnetocrystalline anisotropy energy E_k ($J\cdot m^{-3}$), which is the extra work required to turn the atomic spins from a nearby easy axis to the magnetic field direction, is given, for bcc metals, by the following equation:

$$E_k = K_1(\alpha_1^2\alpha_2^2 + \alpha_2^2\alpha_3^2 + \alpha_3^2\alpha_1^2) + K_2\alpha_1^2\alpha_2^2\alpha_3^2 + K_3(\alpha_1^2\alpha_2^2 + \alpha_2^2\alpha_3^2 + \alpha_3^2\alpha_1^2)^2 + \cdots \quad (2)$$

Where, K_1, K_2, K_3 is the magnetocrystalline anisotropy constant, and α_1, α_2, α_3 are the directional cosines between magnetization intensity M and three crystallographic axes. Usually, only K_1 and K_2 items are considered. Then, the results of calculation are

$$E_{k\langle 110\rangle} = K_1/4,\ (\alpha_1 = \alpha_2 = 1/\sqrt{2}, \alpha_3 = 0);$$
$$E_{k\langle 123\rangle} = K_1/4 + 9K_2/686,\quad (\alpha_1 = 1/\sqrt{14}, \alpha_2 = 2/\sqrt{14}, \alpha_3 = 3/\sqrt{14}).$$

For iron, $K_1(\sim 10^4) > 0$, $K_2(\sim 10^3) < 0$. So the sequence of magnetocrystalline anisotropy energy of grains with different orientations is as follows:

$$E_{k\langle 123\rangle} < E_{k\langle 110\rangle} \quad (3)$$

As a consequence, the changes of magnetic field free energy (ΔG) affecting grains with $\langle 123\rangle$, $\langle 110\rangle$ orientations paralleling to the direction of the magnetic field (MD) can be written in the following sequence:

$$|\Delta G_{\langle 110\rangle}| < |\Delta G_{\langle 123\rangle}| \quad (4)$$

Obviously, the free energy of the nuclei with $\langle 123\rangle$ orientation paralleling to the magnetic field was lower. Thus, they have much larger driving force for nucleation and growth than nuclei with $\langle 110\rangle$ orientations, which might explain why the $\{111\}\langle 123\rangle$ texture component, as compared with $\{111\}\langle 110\rangle$ texture component, was favoured by the magnetic field in the early stage of nucleation and growth.

4. Conclusion

A high magnetic field of 12-tesla was applied during annealing of cold-rolled IF steel sheet with the magnetic field direction paralleling to the rolling direction at 650°C. It was found that the magnetic field annealing retarded the recrystallization process, and favoured the development of $\langle 110\rangle$ texture components at the initial stage of recrystallization. It is worth noting that, as compared with $\{111\}\langle 110\rangle$ texture component, $\{111\}\langle 123\rangle$ texture component was favoured by magnetic field in the early stage of nucleation and growth.

Acknowledgements

This work was supported by the Liaoning Provincial Science and Technology Foundation of China (Grant No. 20051015), the National Science Found for Distinguished Young Scholars (Grant No. 50325102), the key project of National Natural Science Foundation of China (Grant

No. 50234020), the National Natural Science Foundation of China (Grant No. 50501006), and the "111" Project (Grant No. B07015).

The authors would like to appreciate the support of the Center for Materials Analysis and Testing and the High Magnetic Field Laboratory of Northeastern University for providing the facilities.

REFERENCES

1) R. Smoluchowski and R. W. Turner: J. Appl. Phys. **20** (1949) 745–746.
2) V. S. Bhandary and B. D. Cullity: Trans. Metall. Soc. AIME **224** (1962) 1194–1200.
3) H. O. Martikainen and V. K. Lindroos: Scand. J. Metall. **10** (1981) 3–8.
4) T. Watanabe, Y. Suzuki, S. Tani and H. Oikawa: Philo. Mag. Lett. **62** (1990) 9–17.
5) N. Masahashi, M. Matsuo and K. Watanabe: J. Mater. Res. **13** (1998) 457–461.
6) C. S. He, Y. D. Zhang, X. Zhao, L. Zuo, J. C. He, K. Watanabe, T. Zhang, G. Nishijima and C. Esling: Adv. Eng. Mater. **5** (2003) 579–583.
7) C. S. He, Y. D. Zhang, X. Zhao, L. Zuo and C. Esling: Mater. Sci. Forum **495–497** (2005) 465–470.
8) D. A. Molodov, S. Bhaumik, X. Molodova and G. Gottstein: Scripta Mater. **54** (2006) 2161–2164.
9) S. Bhaumik, X. Molodova, D. A. Molodov and G. Gottstein: Scripta Mater. **55** (2006) 995–998.
10) M. Z. Quadir and B. J. Duggan: Acta Mater. **54** (2006) 4337–4350.
11) Y. Y. Tse and B. J. Duggan: Metall. Mater. Trans. **37A** (2006) 1055–1064.
12) F. S. Buffington, K. Hirano and M. Cohen: Acta Metall. **9** (1961) 434–439.
13) H. O. Martikainen and V. K. Lindroos: Scand. J. Metall. **10** (1981) 3–8.
14) S. Nakamichi, S. Tsurekawa, Y. Morizono, T. Watanabe, M. Nishida and A. Chiba: J. Mater. Sci. **40** (2005) 3191–3198.
15) K. Kawahara, Y. Ando, K. Nogiwa, Y. Yagyu, S. Tsurekawa and T. Watanabe: Ann. Chim. Sci. Mat. **27** Suppl 1 (2002) S269–S278.
16) T. Watanabe, S. Tsurekawa, X. Zhao and L. Zuo: Scripta Mater. **54** (2006) 969–975.
17) H. Takechi, H. Katoh and S. Nagishima: Trans AIME **242** (1968) 56–59.
18) N. Rajmohan, Y. Hayakawa, J. A. Szpunar and J. H. Root: Acta Mater. **45** (1997) 2485–2494.
19) W. B. Hutchinson: Acta Metall. **37** (1989) 1047–1056.